PERGAMON

Journal of Structural Geology 21 (1999) 577–583

JOURNAL OF STRUCTURAL GEOLOGY

When do dragfolds not develop into sheath folds in shear zones?

Dazhi Jiang*, Paul F. Williams

Department of Geology, University of New Brunswick, Fredericton, NB, Canada E3B 5A3

Received 4 June 1998; accepted 1 March 1999

Abstract

Using a unified model for high-strain zones, rotation paths of material lines in different flow types are investigated and presented as stereographic projections. A material fabric element such as a mineral lineation or a fold axis can be plotted on such stereograms and the rotation path revealed. Using this method, we examine the rotation of folds and the development of sheath folds in general three-dimensional zonal deformation. We show that the evolution of dragfold geometry in a high-strain zone depends on the flow type and the initial perturbation of the fold axis. In simple shear zones and thickening zones (monoclinic or triclinic), dragfolds will evolve into sheath folds. In monoclinic thinning zones with biaxially stretching boundaries, if the shear direction is parallel to the maximum stretching direction of the boundary, sheath folds will develop. If the shear direction is parallel to the minimum stretching direction of the boundary, dragfolds become more cylindrical as deformation advances. In thinning zones with boundaries equally stretched in all directions, the likelihood of sheath fold development depends on the ratio of the shear strain rate to the thinning rate. In triclinic thinning zones, fold evolution depends on the details of the flow and the value of initial fold axis perturbation.

1. Introduction

By the end of the 1970s, it was generally accepted that dragfolds may be progressively rotated by simple shear towards parallelism with the shear direction (Bryant and Reed, 1969; Escher and Watterson, 1974; Hobbs et al., 1976, p. 287). It was then realized that, under certain conditions, opposite ends of a single fold hinge may rotate in opposite senses to produce a sheath fold (not all early authors use the term 'sheath fold') (Howard, 1968; Carreras et al., 1977; Rhodes and Gayer, 1977; Williams and Zwart, 1977; Bell, 1978; Quinquis et al., 1978; Cobbold and Quinquis, 1980). Skjernaa (1989) claimed that some tight sheath folds observed in nature (e.g. Hansen, 1971; Williams and Zwart, 1977; Henderson, 1981) may not be explained by simple shear alone. Despite this and the recognition that natural high-strain zones may deviate significantly from simple shear (Ramberg, 1975; Hobbs et al., 1976, pp. 266 and 300; Sanderson and Marchini, 1984; Hanmer and Passchier, 1991; Fossen and Tikoff, 1993; Simpson and De Paor, 1993) or even from monoclinic symmetry (Robin and Cruden, 1994; Jiang and Williams, 1998; Lin et al., 1998; Jiang, 1999), it has been tacitly assumed that the simple shear model is generally applicable. An important observation, from both the literature and our own experience that requires explanation, is that sheath folds are common only in some high-strain zones but are very rare or even absent from others, even though, in such zones, fold hinges may be generally rotated towards parallelism with the stretching lineation. Areas such as the Chedabucto Fault in Nova Scotia, Canada, and the Monashee complex in the Canadian Cordillera have all the characteristics of high-strain zone deformation, yet very few or no sheath folds are developed despite the fact that fold axes have been rotated (Mawer and Williams, 1991; McNicoll and Brown, 1994). Further, the folds all have the same asymmetry, either all s- or all z-folds.

The occurrence of sheath folds is not haphazard, although many factors affect the evolution of folds in high-strain zones, including the initial fold geometry with respect to the flow, the flow characteristics and

* Corresponding author.
E-mail address: dzjiang@unb.ca (D. Jiang)

0191-8141/99/$ - see front matter
PII: S0191-8141(99)00065-6

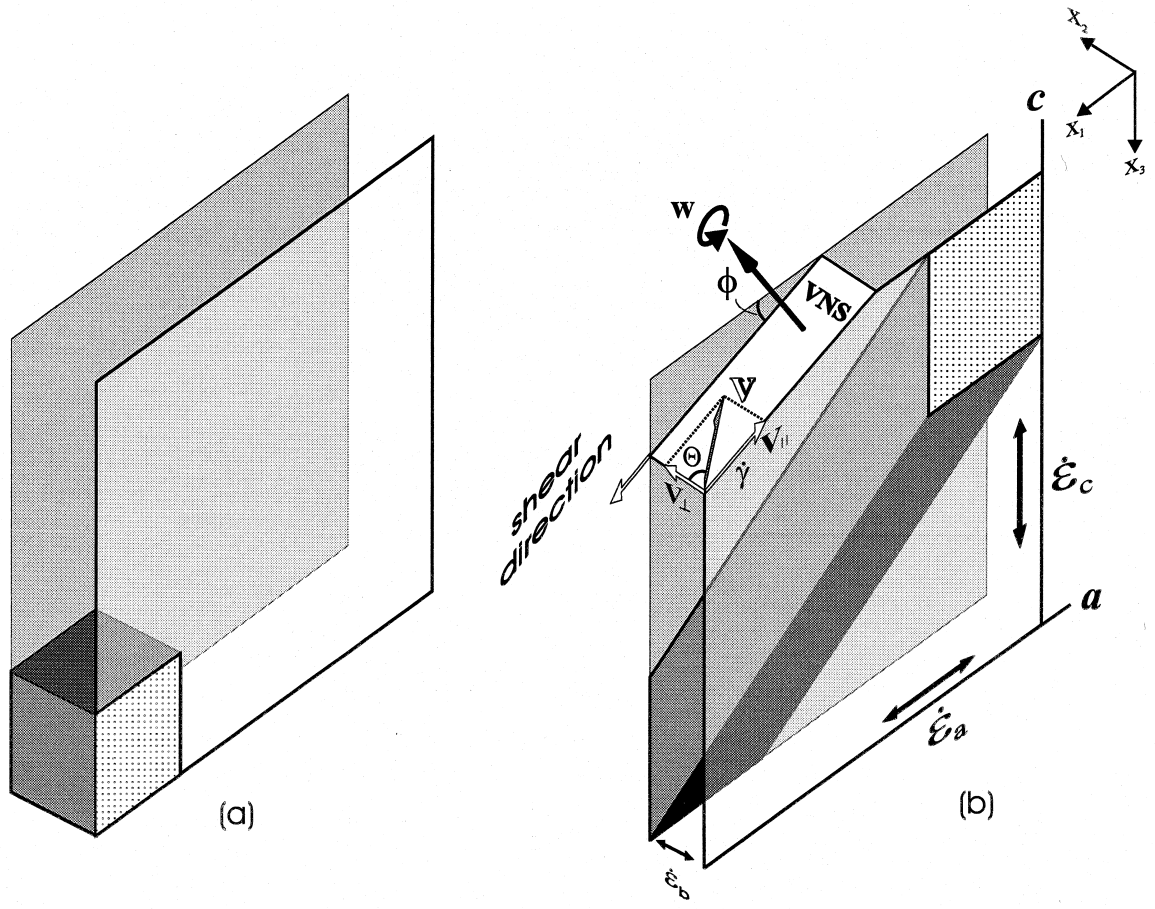

Fig. 1. Nomenclature used in the text to describe a high-strain zone. (a) The undeformed configuration. (b) The deformed configuration resulting from a general triclinic non-coaxial deformation path. The boundaries of the zone undergo biaxial stretching with the minimum rate-of-stretch ($\dot{\epsilon}_a$) and maximum rate-of-stretch ($\dot{\epsilon}_c$) parallel to the *a* and *c* directions, respectively. The relative velocity, *v*, of one boundary (front) with respect to the other (back) makes an angle Θ with respect to the boundary normal. It is decomposed into a boundary-normal component, $v_\perp$, leading to thinning or thickening of the zone ($\dot{\epsilon}_b$), and a boundary-parallel component, $v_{||}$, leading to shearing which makes an angle ϕ with the *a* direction. VNS stands for vorticity-normal section. $x_1x_2x_3$ is the reference frame used to define the flow.

the history of flow. We investigate the influence of flow characteristics in high-strain zones on the evolution of dragfolds—folds which initiate in layers parallel to the zone boundaries in response to vorticity, with their axes parallel to the vorticity vector (e.g. Lister and Williams, 1983). Our work therefore extends the existing sheath fold development model based on simple shear (e.g. Williams and Zwart, 1977; Quinquis et al., 1978; Cobbold and Quinquis, 1980) to general three-dimensional deformation conditions including triclinic deformation paths. We show that both the likelihood for dragfolds to develop into sheath folds and the geometrical relationship between the final folds and other fabric elements, such as lineations, vary with flow type. Folds other than dragfolds can develop in high-strain zones with their initial axes most likely dependent on the sectional flow in the plane of the layer (Treagus and Treagus, 1981, 1992; James and Watkinson, 1993; Jiang, 1999). There may also be folds that are inherited from pre-high-strain zone deformation. Given the right geometry and flow type, these folds may also develop into sheath folds. There are an infinite variety of possibilities with non-dragfolds. We only consider dragfolds in this paper, but the method introduced here can be used to investigate any fold axis rotation once the initial geometry of the fold and the flow type are determined.

2. Flow in high-strain zones

A general high-strain zone can be considered as a zone with biaxially-stretching boundaries plus a shear on the boundary that is oblique to the principal stretching directions of the boundaries (Fig. 1; Jiang and Williams, 1998). The two principal rate-of-stretch directions of the boundaries are referred to as the *a* and *c* directions, respectively, with strain rates $\dot{\epsilon}_a$ and $\dot{\epsilon}_c$ ($|\dot{\epsilon}_a| \leq |\dot{\epsilon}_c|$ by definition). The strain rate along the zone boundary normal is denoted $\dot{\epsilon}_b$. The shear direc-

tion makes an angle ϕ with respect to the a direction and the shear strain rate is denoted $\dot{\gamma}$ (Fig. 1). In the reference frame, $x_1x_2x_3$, established such that x_1 and x_3 are parallel to a and c, respectively, and x_2 is perpendicular to the zone boundary (Fig. 1), the relative velocity vector of the two zone boundaries $\mathbf{v}$, making an angle Θ with respect to the zone normal (x_2), is decomposed into a boundary-parallel component ($\mathbf{v}_{\|}$), which leads to shearing within the zone, and a boundary-normal component ($\mathbf{v}_{\perp}$) (Fig. 1). $\dot{\epsilon}_b$ and $\dot{\gamma}$ can be related to the velocity by (Jiang and Williams, 1998, eq. 4):

$$\dot{\gamma} = \frac{\partial v}{\partial x_2}\sin\Theta,\ \dot{\epsilon}_b = \frac{\partial v}{\partial x_2}\cos\Theta. \tag{1}$$

Normalizing $\dot{\epsilon}_a$ and $\dot{\epsilon}_c$ with respect to $\dot{\epsilon}_b$ for simpler presentation, we define a and c according to:

$$a = -\dot{\epsilon}_a/\dot{\epsilon}_b,\ c = -\dot{\epsilon}_c/\dot{\epsilon}_b. \tag{2}$$

The velocity gradient tensor, $\mathbf{L}$, for the flow within a general high-strain zone can thus be expressed as (cf. Jiang and Williams, 1998, eq. 5):

$$\mathbf{L} = \left|\frac{\partial v}{\partial x_2}\right| \begin{pmatrix} a\cdot\cos\Theta & \sin\Theta\cdot\cos\phi & 0 \\ 0 & b\cdot\cos\Theta & 0 \\ 0 & \sin\Theta\cdot\sin\phi & c\cdot\cos\Theta \end{pmatrix}, \tag{3}$$

where b can have values of -1, 0, or 1. $b=-1$ represents a *thinning zone* where the two material boundaries of the zone are moving toward each other, $b=0$ a *constant-thickness zone* where the two material boundaries maintain the same spacing, and $b=1$ a *thickening zone* where the two boundaries are moving away from each other. The terms are chosen to distinguish these zones from the widening and narrowing zones of Means (1995) where the zone boundaries migrate through the material. Thickening and thinning zones have boundaries that do not migrate through the material (i.e. they are attached to the same material planes) but move further or closer to one another in response to zone-normal stretching. Thickening and thinning are not incompatible with widening and narrowing and, for example, a thickening zone may be widening or narrowing.

In any flow there are spatial orientations called flow apophyses (Ramberg, 1975) parallel to which material lines do not rotate. These spatial orientations are eigenvectors of $\mathbf{L}$. The flow depicted in Eq. (1) generally has three apophyses $\mathbf{A}_1$, $\mathbf{A}_2$ and $\mathbf{A}_3$ with stretchings along them, A_1, A_2 and A_3. A_1, A_2 and A_3 can have any magnitude, but in this paper, $A_1 \geq A_2 \geq A_3$ by definition in order to avoid redundant treatment of flow. Depending on the behavior of material lines in the vicinity of apophyses, they have been called attractors, transits or repulsors of material lines (Passchier, 1997). For the flow described in Eq. (1), two of the apophyses correspond to a and c. For a thinning zone ($b=-1$), $\mathbf{A}_1$ and $\mathbf{A}_2$ are parallel to c and a, respectively and $\mathbf{A}_3$ is inclined to the ac-plane. For a thicken-

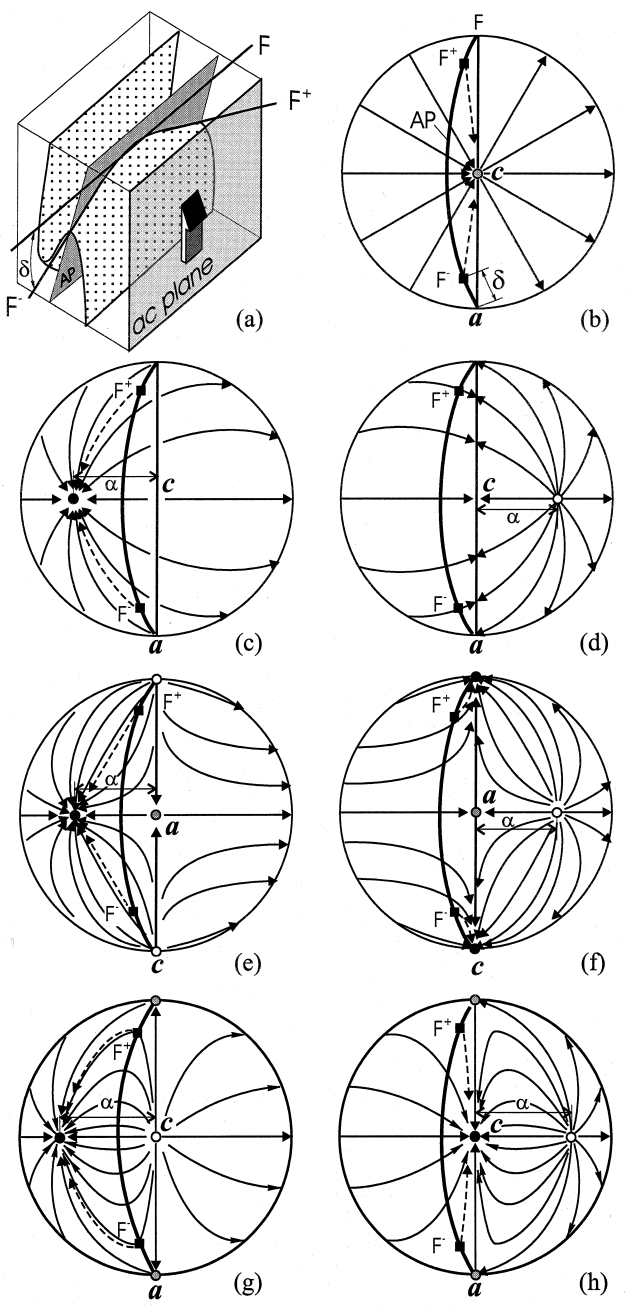

Fig. 2. Evolution of dragfold geometry in monoclinic flow. (a) Block diagram showing the initial configuration of a dragfold. F is the mean fold axis with initial perturbations δ giving F^+ $(F+\delta)$ and F^- $(F-\delta)$ within the axial plane (AP) of the fold. The shear direction is set vertical. (b)–(h) Lower hemisphere stereographic projections of the rotation loci (solid arrows) of material lines for different types of monoclinic flows. (c), (e) and (g) are thickening zones and (d), (f) and (h) are thinning zones. Black, shaded and blank circles in the stereograms represent flow apophyses $\mathbf{A}_1$, $\mathbf{A}_2$ and $\mathbf{A}_3$, respectively. Dashed arrows represent progressive rotation of F^+ and F^-. See text for further discussion.

ing zone ($b = 1$) $\mathbf{A}_3$ and $\mathbf{A}_2$ are parallel to c and a, respectively and $\mathbf{A}_1$ is inclined to the ac-plane. Simple shear flow is the special case where $A_1 = A_2 = A_3 = 0$ and $\mathbf{A}_1$, $\mathbf{A}_2$ and $\mathbf{A}_3$ all lie in the shear plane.

The flow varies in symmetry depending on the values of a, c, Θ and ϕ in Eq. (1). $\Theta = 0$ is the situation of pure shear and the symmetry of the flow is orthorhombic or higher. The symmetry of the flow becomes monoclinic when any one of the following conditions are met: $\Theta = 90^\circ$, $a = c$, $\phi = 0^\circ$ and $\phi = 90^\circ$. The flow is triclinic when $a<c$ and $0^\circ<\phi<90^\circ$. We now investigate the evolution of fold geometry for all these different flow situations.

3. Dragfold evolution in monoclinic flows

Consider a layer parallel to a high-strain zone boundary (ac-plane) and the initiation of dragfolds in the layer (Fig. 2a). Supposing that the shear direction is vertical, the initial folds have approximately horizontal axes (F parallel to the vorticity vector) and axial planes (AP) close to the XY plane of the infinitesimal strain ellipsoid. As deformation advances, the axial planes will rotate towards parallelism with $\mathbf{A}_1$ and the folds become progressively tighter. The fold axes F have inevitable initial perturbations δ within their axial planes giving F^+ $(= F + \delta)$ and F^- $(= F - \delta)$, i.e. they are curved within their axial planes. Because of this initial orientation difference, F^+ and F^- may rotate differently in the flow field giving rise to various final fold geometries (Fig. 2). The rotation loci of material lines can be calculated by using the position gradient tensor, the finite deformation counterpart of Eq. (1), given in Jiang and Williams (1998, eq. 14). We have assumed the orientation for Fig. 2 to facilitate description but the treatment and conclusions are independent of orientation. Monoclinic high-strain zones fall into the following four types.

3.1. $\Theta = 90^\circ$ (simple shear, Fig. 2b)

Fig. 2(b) shows the rotation loci of material lines in a simple shear flow by means of a stereogram. The fold axes F, F^+, F^- and the axial plane are plotted on the stereogram. It is seen from the stereogram that F^+ and F^- will rotate (indicated by dashed arrows) away from F towards parallelism thus resulting in sheath fold development as deformation progresses. The tightness and final geometrical shape of the sheath fold will depend on the magnitude of finite strain. It is generally true in all situations that the magnitude of fold axis rotation is a function of the magnitude of finite strain.

3.2. $a = c$ (Fig. 2c and d)

This is the situation where the boundaries of the zone are being stretched or shortened (negative stretching) equally in all directions (the strain ellipse on the boundary is an expanding or shrinking circle). For a thickening zone (Fig. 2c), $A_2 = A_3<0$ and both lie in the ac-plane, $A_1 > 0$ and lies in the VNS making an angle α $(= \cos^{-1} W_k^s)$ with the ac-plane, where W_k^s is the sectional kinematic vorticity in the VNS (Fig. 1). The whole ac-plane forms a material line repulsor plane (Passchier, 1997) and because $A_2 = A_3$, these apophyses have no specific orientation within the plane. $\mathbf{A}_1$ is an attractor. For a thinning zone (Fig. 2d), $A_1 = A_2 > 0$ and both lie in the ac-plane, $A_3<0$ and lies in the VNS making an angle α $(= \cos^{-1} W_k^s)$ with the ac-plane. The ac-plane forms a material line attractor plane (Passchier, 1997). The progressive rotation of dragfold axes (F^+, F^-) is different for thickening and thinning zones. In a thickening zone, the fold axes rotate away from the ac-plane (repulsor) towards $\mathbf{A}_1$ via a great circle path and result in sheath folds (Fig. 2c). In a thinning zone, the axes rotate towards the ac-plane (attractor) via a great circle path (Fig. 2d). Whether or not sheath folds develop depends solely on α, the angle between $\mathbf{A}_3$ and the ac-plane, which in turn is related to the sectional kinematic vorticity number, W_k^s. The smaller the angle (a higher W_k^s), the closer Fig. 2(d) resembles Fig. 2(b) and the more likely sheath folds are to develop.

3.3. $a<c$ and $\phi = 0^\circ$ (Fig. 2e and f)

In this situation, the boundaries are stretched (or shortened, negative stretch) biaxially with different rates of stretch parallel to a and c and the shear is parallel to a. The transpression zone of Sanderson and Marchini (1984) is a special thinning zone example of this situation. Again, fold axis rotation is different depending on whether the zone is thickening or thinning. In a thickening zone, F^+ and F^- rotate towards $\mathbf{A}_1$ forming sheath folds (Fig. 2e). If the zone is thinning, the initial perturbated fold axes F^+ and F^- will rotate towards F as strain advances and therefore towards coincidence. Instead of developing into sheath folds, the folds become more cylindrical as deformation increases (Fig. 2f).

3.4. $a<c$ and $\phi = 90^\circ$ (Fig. 2g and h)

This situation is identical to Section 3.3 except that the shear is parallel to c. A thrusting zone with boundaries stretched along the transport direction is an example of a thinning zone. The initially perturbed fold axes F^+ and F^- rotate away from the mean (F)

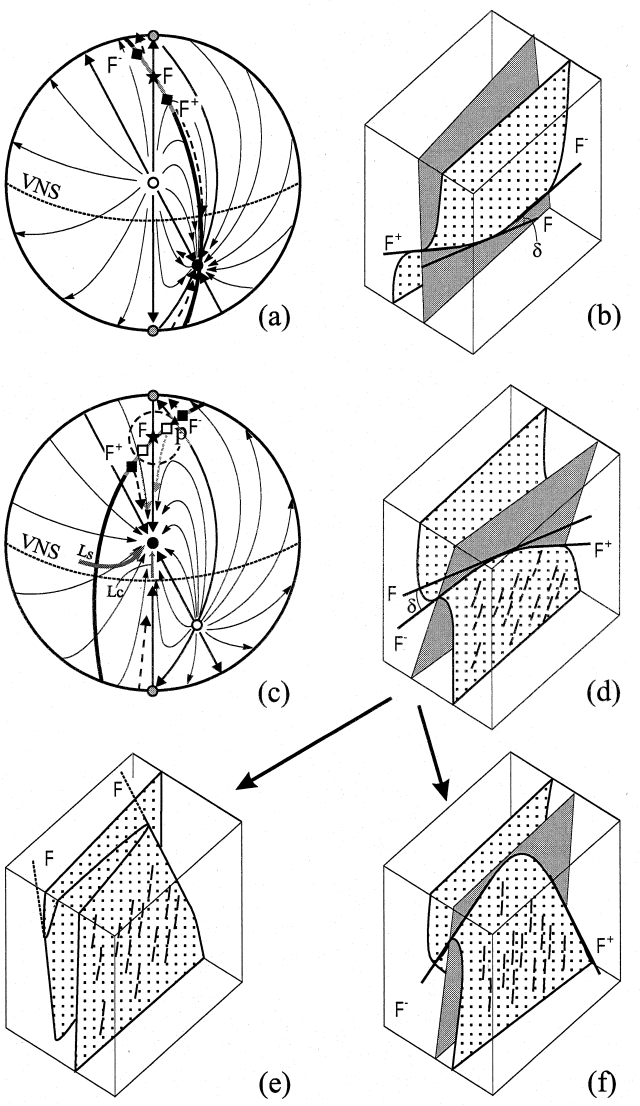

Fig. 3. Dragfold evolution in a triclinic thickening zone (a and b) and triclinic thinning zone (c–f). (a) Stereogram showing the loci of rotation of material lines (symbols as in Fig. 2) for a thickening zone. (b) Initial configuration of a dragfold in a thickening zone. Sheath fold will develop. (c) Stereogram showing the loci of rotation of material lines for a thinning zone. Depending on details of the flow and the initial fold axis curvature, the fold will evolve different geometries. (d) Initial configuration of a dragfold in a thinning zone. (e) The situation with no sheath fold development. (f) The situation producing sheath folds. Ls and Lc in (c) are loci of finite-strain-related lineation and slickenside striae lineations. Short lines in (d), (e) and (f) schematically represent finite-strain-related lineations (e.g. mineral lineations). See text for further discussion.

orientation and produce sheath folds in both thickening (Fig. 2g) and thinning zones (Fig. 2h).

4. Dragfold evolution in triclinic flows

For a general case [i.e. $a<c$ and $0^\circ<\phi<90^\circ$ in Eq. (1)], the flow is triclinic. a and c remain two apophyses and the orientation of the inclined apophysis ($\mathbf{A}_3$ for a thinning zone and $\mathbf{A}_1$ for a thickening zone) can be calculated by taking the eigenvectors of Eq. (1). Dragfold evolution depends on the values of Θ, ϕ, a and c because they determine the orientations of flow apophyses.

Fig. 3(a) presents the flow apophyses and the rotation loci of material lines in a thickening zone with $a=0$, $c=1$, $\Theta=75^\circ$ and $\phi=60^\circ$. Fig. 3(b) shows the corresponding initial configuration of a dragfold. Progressive rotation of fold axes will produce sheath folds (Fig. 3a). In a triclinic thinning zone however, fold evolution depends on the flow properties (the values of a, c, Θ and ϕ) and the magnitude of the initial perturbation of fold axes as demonstrated in Fig. 3(c–f). Fig. 3(c) is the material line rotation loci map for a thinning zone with $a=0$, $c=1$, $\Theta=75^\circ$ and $\phi=60^\circ$. Fig. 3(d) shows the initial configuration of a dragfold pair with fold axes F parallel to the vorticity vector. The initial axial plane intersects the $\mathbf{A}_2\mathbf{A}_3$-plane at $\mathbf{p}$ (black triangle in Fig. 3c). The angle between F and $\mathbf{p}$ in the axial plane is denoted σ and a small circle of angular radius σ and center F can be defined (dashed line circle, Fig. 3c). If F^+ and F^- lie within the small circle (i.e. $\delta<\sigma$) they will rotate with the same sense towards $\mathbf{A}_1$ and no sheath fold will form (Fig. 3e). If F^+ and F^- lie outside the small circle (i.e. $\delta\geq\sigma$) they will have opposite senses of rotation and will produce sheath folds (Fig. 3f). The orientation of ridge-in-groove slickenside striae (Lc) (Means, 1987; Lin and Williams, 1992) and rotation loci for finite-strain-related lineation (Ls) are also shown in Fig. 3(c–f). Unlike monoclinic situations where lineations are symmetrically distributed with respect to the fold (parallel to fold axes or bisecting the two branches of a sheath fold), in triclinic situations, the lineations are 'oblique' to the fold axes as shown schematically in Fig. 3(e) and (f). Where a sheath fold develops, it is commonly asymmetrical and the lineations may intersect one branch with a smaller angle than with the other branch (see fig. 4A of Carreras et al., 1977). Where there are no sheath folds, the lineations usually exhibit an angular relationship with the fold axes and are consistently on one side of the fold axes as we observe in the Monashee Complex (see also fig. 8, McNicoll and Brown, 1994).

5. Discussion and conclusions

Dragfolds are likely to be converted to sheath folds in shear zones with simple shear deformation paths and also in monoclinic or triclinic thickening zones considered in this paper. The strain of the thickening zone types considered in this paper is constrictional (fig. 12, Jiang and Williams, 1998). This agrees with

Fletcher and Bartley (1994) and Fletcher et al. (1995) who have concluded that sheath folds are more likely to develop in constrictional non-coaxial shear zones. For thinning zones with monoclinic symmetries, only the situation where the shear direction is parallel to the maximum stretching direction of the boundary favors sheath fold development. If the shear direction is parallel to the minimum stretching direction of the boundary, dragfolds become more cylindrical as deformation advances. Therefore, in a transcurrent shear zone with vertical stretching > strike-parallel stretching, such as the transpression zone of Sanderson and Marchini (1984), one would not expect dragfolds to evolve into sheath folds. If a thinning zone has boundaries equally stretched in all directions, fold evolution depends on the sectional kinematic vorticity number. The closer it is to unity (simple shear) the more sheath folds are likely to develop. In a triclinic thinning zone, fold evolution depends on the details of the flow and the value of the initial fold axis perturbation, as explained in Fig. 3(c–f).

Not all folds in high-strain zones develop as dragfolds as mentioned in the introduction. They may also develop by buckling of layers or dykes inclined to the shear zone in such a way that their intersection with the shear plane, and hence the resulting fold hinelines, are not parallel to the vorticity vector. In this case the resultant geometry reflects their initial asymmetry with respect to the flow. However, once the initial geometry of a fold is determined, its successive rotation can be investigated by means of the rotation loci map. Two problems with this approach are: (i) fold axis rotation may not be passive (Mawer and Williams, 1991); and (ii) flow may be non-steady and the kinematics may change continuously (Williams and Compagnoni, 1977; Jiang and White, 1995). All of these factors may contribute to a particular observed geometry and it can be difficult, if not impossible, to identify. However, by examining all existing fabric elements including indicators of vorticity, non-coaxiality and displacement, better constraints on the natural deformation are possible. For example the consistent obliquity between the fold and lineation and lack of sheath folds in a high-strain zone where fold axes have rotated may suggest that the deformation path was triclinic.

Acknowledgements

We thank Drs John Fletcher, Michael Williams and Peter Hudleston for their thoughtful reviews, and Shoufa Lin and Richard Brown for discussion. The paper was written while DJ held a Post-doctoral Fellowship from the Natural Sciences and Engineering Research Council of Canada (NSERC). Support by NSERC through a research grant to PFW is also acknowledged.

References

Bell, T.H., 1978. Progressive deformation and reorientation of fold axes in a ductile mylonite zone: the Woodroffe thrust. Tectonophysics 44, 285–320.

Bryant, B., Reed, J.C., 1969. Significance of lineation and minor folds near major thrust faults in the southern Appalachian and the British and Norwegian Caledonides. Geological Magazine 106, 412–429.

Carreras, J., Estrada, A., White, S., 1977. The effects of folding on the *c*-axis fabrics of a quartz mylonite. Tectonophysics 39, 3–24.

Escher, A., Watterson, J., 1974. Stretching fabrics, folds and crustal shortening. Tectonophysics 22, 223–231.

Fletcher, J.M., Bartley, J.M., 1994. Constrictional strain in a non-coaxial shear zone; implications for fold and rock fabric development, central Mojave metamorphic core complex, California. Journal of Structural Geology 16, 555–570.

Fletcher, J.M., Bartley, J.M., Martin, M.W., Glazner, A.F., Walker, J.D., 1995. Large-magnitude continental extension, an example from the central Mojave metamorphic core complex. Geological Society of America Bulletin 107, 1468–1483.

Fossen, H., Tikoff, B., 1993. The deformation matrix for simultaneous simple shearing, pure shearing and volume change, and its application to transpression–transtension tectonics. Journal of Structural Geology 15, 413–422.

Hanmer, S.K., Passchier, C.W., 1991. Shear-sense indicators: a review. Geological Survey of Canada Paper 90-17.

Hansen, E., 1971. Strain Facies. Springer-Verlag, New York.

Henderson, J.R., 1981. Structural analysis of sheath folds with horizontal *X*-axis, northeast Canada. Journal of Structural Geology 3, 203–210.

Hobbs, B.E., Means, W.D., Williams, P.F., 1976. An Outline of Structural Geology. John Wiley, New York.

Howard, K.A., 1968. Flow direction in triclinic folded rocks. American Journal of Sciences 266, 758–765.

James, A.I., Watkinson, A.J., 1993. Initiation of folding and boudinage in wrench shear and transpression. Journal of Structural Geology 16, 883–893.

Jiang, D., 1999. Vorticity decomposition and its application to sectional flow characterization. Tectonophysics 301 243–259.

Jiang, D., White, J.C., 1995. Kinematics of rock flow and the interpretation of geological structures, with particular reference to shear zones. Journal of Structural Geology 17, 1249–1265.

Jiang, D., Williams, P.F., 1998. High-strain zones: a unified model. Journal of Structural Geology 20, 1105–1120.

Lin, S., Williams, P.F., 1992. The origin of ridge-in-groove slickenside striae and associated steps in an *S–C* mylonite. Journal of Structural Geology 14, 315–321.

Lin, S., Jiang, D., Williams, P.F., 1998. Transpression (or transtension) zones of triclinic symmetry: natural example and theoretical modelling. In: Holdsworth, R.E, Strachan, R.A, Dewey, J.F (Eds.), Continental Transpression and Transtension Tectonics, 135. Geological Society Special Publication, pp. 41–57.

Lister, G.S., Williams, P.F., 1983. The partitioning of deformation in flowing rock masses. Tectonophysics 92, 1–33.

McNicoll, V.J., Brown, R.L., 1994. The Monashee décollement at Cariboo Alp, southern flank of the Monashee complex, southern British Columbia, Canada. Journal of Structural Geology 16, 17–30.

Mawer, C.K., Williams, P.F., 1991. Progressive folding and foliation development in a sheared, coticule-bearing phyllite. Journal of Structural Geology 13, 539–555.

Means, W.D., 1987. A newly recognized type of slickenside striation. Journal of Structural Geology 9, 585–590.

Means, W.D., 1995. Shear zones and rock history. Tectonophysics 247, 157–160.

Passchier, C.W., 1997. The fabric attractor. Journal of Structural Geology 19, 113–127.

Quinquis, H., Audren, C.L., Brun, J.P., Cobbold, P.R., 1978. Intense progressive shear in the Ile de Groix blueschists. Nature 273, 43–45.

Ramberg, H., 1975. Particle paths, displacement and progressive strain applicable to rocks. Tectonophysics 28, 1–37.

Rhodes, S., Gayer, R.A., 1977. Non-cylindrical folds, linear structures in the X direction and mylonite developed during translation of the Caledonian Kalak Nappe Complex of Finnmark. Geological Magazine 114, 329–341.

Robin, P.-Y.F., Cruden, A.R., 1994. Strain and vorticity patterns in ideally ductile transpressional zones. Journal of Structural Geology 16, 447–466.

Sanderson, D.J., Marchini, W.R.D., 1984. Transpression. Journal of Structural Geology 6, 449–458.

Simpson, C., De Paor, D.G., 1993. Strain and kinematic analysis in general shear zones. Journal of Structural Geology 15, 1–20.

Skjernaa, L., 1989. Tabular folds and sheath folds: definitions and conceptual models for their development, with examples from the Grapesvare area, northern Sweden. Journal of Structural Geology 11, 689–703.

Treagus, J.E., Treagus, S.H., 1981. Folds and the strain ellipsoid: a general model. Journal of Structural Geology 3, 1–17.

Treagus, S.H., Treagus, J.E., 1992. Transected folds and transpression: how are they related? Journal of Structural Geology 14, 361–367.

Williams, P.F., Zwart, H.J., 1977. A model for the development of the Seve–Köli Caledonian Nappe Complex. In: Saxena, S.K, Bhattacharji, S (Eds.), Energetics of Geological Processes. Springer-Verlag, New York, pp. 169–187.